Tetrahedron 69 (2013) 7653–7658

Contents lists available at SciVerse ScienceDirect

Tetrahedron

journal homepage: www.elsevier.com/locate/tet

Structure–activity relationships of small molecule inhibitors of RAGE-Aβ binding

Nathan T. Ross [a], Rashid Deane [b,c], Sheldon Perry [b], Benjamin L. Miller [a,d,*]

[a] Department of Biochemistry and Biophysics, University of Rochester, Rochester, NY 14642, USA
[b] Center of Neurodegernerative and Vascular Brain Disorders, University of Rochester, Rochester, NY 14642, USA
[c] Center for Translational Neuromedicine, University of Rochester, Rochester, NY 14642, USA
[d] Department of Dermatology, University of Rochester, Rochester, NY 14642, USA

ARTICLE INFO

Article history:
Received 28 February 2013
Received in revised form 18 May 2013
Accepted 20 May 2013
Available online 24 May 2013

Keywords:
Receptor for advanced glycation endproducts
Amyloid beta peptide
Focused library
Alzheimer's disease

ABSTRACT

The Receptor for Advanced Glycation Endproducts ('RAGE') mediates transport of amyloid-β peptide (Aβ) into the brain, and is therefore an important target for the development of therapeutic agents for Alzheimer's disease. We describe structure–activity relationships for inhibition of RAGE-Aβ binding, derived from the analysis of a library of tertiary amides.

1. Introduction

Demographic changes and longer life spans have combined to steadily increase the number of people afflicted with Alzheimer's disease, and this trend is predicted to continue.[1] Given that current estimates put the global prevalence of dementia at 24 million,[2] the development of new therapeutic strategies for Alzheimer's disease is therefore an urgent challenge to the chemistry community.

The amyloid hypothesis holds that Alzheimer's disease results from the accumulation of amyloid-β peptide (Aβ) in the brain.[3] Many targets have been explored as potential anti-Alzheimer's therapeutic strategies,[4] including β-[5] and γ-[6] secretase inhibitors, Aβ-targeted immunotherapy,[7] and interference with the formation of neuronal tangles consisting of aggregates of hyperphosphorylated tau protein.[8] Recent work suggests that protein kinase C may be an important player in Alzheimer's pathology as well.[9] While all of these have produced exciting results in in vitro assays and in some cases have progressed as far as human clinical trials, none has yet yielded an FDA-approved drug.

An emerging target for anti-Alzheimer's drug development is the Receptor for Advanced Glycation Endproducts (RAGE). A member of the immunoglobulin superfamily,[10] RAGE binds a broad range of ligands via its extracellular V domain. In addition to the advanced glycation endproduct (AGE) proteins from which RAGE gets its name, these include the S100 family of proteins, amphoterin/HMGB1, and, the particular focus of this research, Aβ. RAGE is upregulated in the brain vasculature of Alzheimer's disease,[11] and mediates transport of Aβ across the blood–brain barrier.[12]

We recently reported the results of a high-throughput screen for inhibitors of RAGE-Aβ binding that yielded compounds **2**–**4** as 'hits'.[13] Analysis of the structural features of these compounds led to the synthesis of a focused library of compounds designed based on a common pharmacophore hypothesis. One compound selected from this library, **1**, was found to inhibit RAGE-Aβ binding in vitro, and dramatically decreased the brain accumulation of Aβ in a mouse model of Alzheimer's disease. Since our initial report, 2-aminopyrimidine derivatives[14] and trisubstituted thiazoles[15] with the ability to disrupt RAGE-Aβ binding have been reported. Here, we provide a detailed discussion of the design, synthesis, and activity of the full focused library, and an analysis of the structural features underlying inhibition of RAGE-Aβ binding.

2. Results and discussion

As described previously,[13] a commercial diversity library of 5000 compounds (Comgenex) was assayed for the ability to disrupt RAGE-Aβ interaction using RAGE transfected CHO (Chinese hamster

* Corresponding author. Tel.: +1 585 275 9805; fax: +1 585 273 1346; e-mail address: benjamin_miller@urmc.rochester.edu (B.L. Miller).

0040-4020/$ – see front matter © 2013 Elsevier Ltd. All rights reserved.
http://dx.doi.org/10.1016/j.tet.2013.05.079

ovary) cells and I^{125}-Aβ. The three most active 'hit' compounds identified from this screen have a central tertiary amide core, an electron rich aromatic group, a hydrophobic group, and two of the three have electron deficient aromatic rings (Fig. 1). Based on the similarity between these compounds a focused library was designed that could be readily assembled in parallel using commercially available building blocks. The library contained building blocks representing the three similar peripheral functionalities of the previous hits: an electron rich aromatic group, a hydrophobic group, and an electron deficient benzene. Building blocks were chosen with an eye toward reducing molecular weight relative to **2**–**4**, while providing structures with the common features seen in these molecules. The 100-compound library (supplemental Fig. 1) was assembled using Borch reductive amination[16] followed by parallel acetylation (Scheme 1).

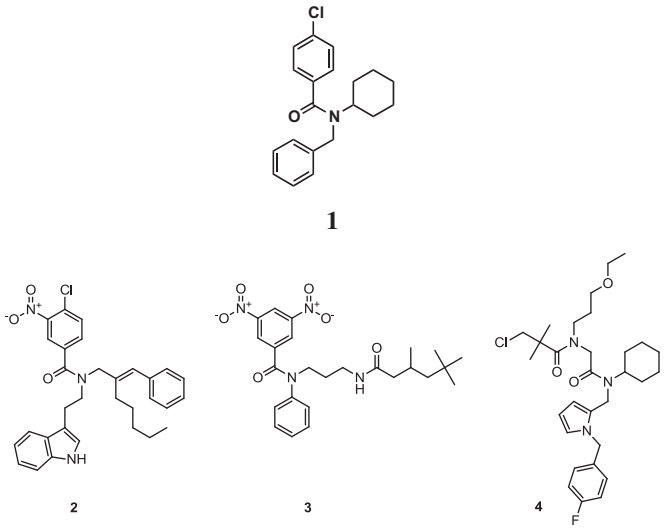

Fig. 1. Hit compounds from a high-throughput screen for modulators of the RAGE-Aβ interaction.

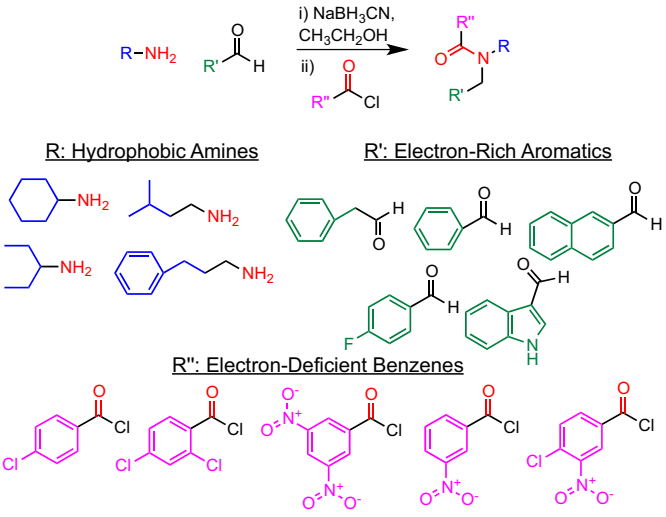

Scheme 1. Synthetic scheme for library generation, and library building blocks.

Following synthesis, library members were purified to an average purity of >95% by reverse phase HPLC, and screened in RAGE transfected CHO cells for their ability to block I^{125}-Aβ peptide binding. A binding index for Aβ was determined in the presence and absence of compound, where:

$$\text{Binding Index}_{A\beta} = \frac{[\text{RAGE bound } I^{125}A\beta]}{[I^{125}A\beta \text{ in medium}]} \times [A\beta_{\text{Total}}]$$

Subtracting the binding index obtained in the presence of compound from the binding index in the absence of compound provided a differential binding index; inhibition of RAGE-Aβ binding yields a differential binding index >0.

A broad range of compound activities were observed in the primary screening assay, with five compounds from the library performing as well or better than the best hits from the initial library screen (Fig. 2).

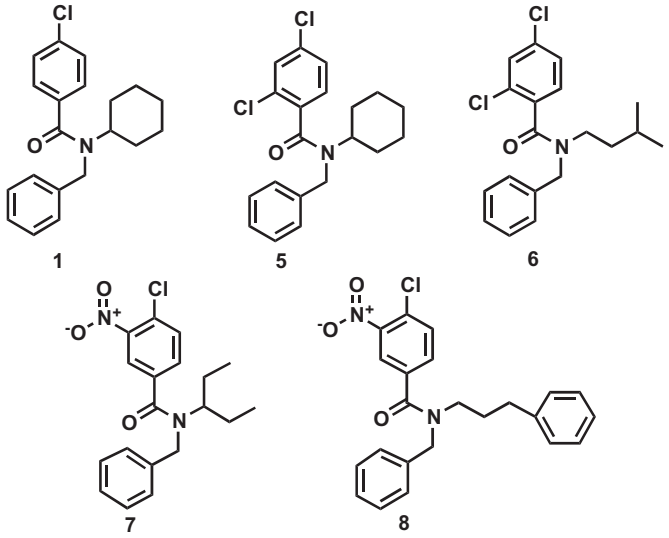

Fig. 2. Top hits from the 100-compound focused library.

Since various portions of a molecule may contribute synergistically to binding (or may antagonize one another), examination of individual building blocks is an oversimplification, but still useful in establishing an overall picture of the SAR. To that end, Figs. 3–5 show screening data sorted by building block class (hydrophobic amine, electron rich aromatic, electron poor benzene). Ability to inhibit RAGE-Aβ binding is reported on the *y*-axis as a differential binding index, as described above.

The strongest structure–activity correlation was observed for the electron rich aromatic group (R′ in Scheme 1; Fig. 3). When the benzaldehyde building block was used, compounds were on average more than two times more active than the average performance of all library members. All five of the compounds with the strongest ability to inhibit RAGE-Aβ binding incorporated this building block. This result is particularly striking when compared with the average inhibitory potency of compounds incorporating either the 4-fluorobenzaldehyde or phenylacetaldehyde building blocks. Conversely, the indole containing electron rich aromatic was deleterious to binding; no compounds containing this functionality had significant activity in the assay. Examination of structure–activity relationships for the hydrophobic amine (R in Scheme 1; Fig. 4) and electron deficient benzene (R″ in Scheme 1; Fig. 5) groups suggests that RAGE tolerates a significant amount of structural variation in these portions of the molecule. However, chloro substitution of the electron deficient benzene was generally more favorable than nitro substitution. As can be seen from surface electrostatic potential maps generated from density functional calculations at the B3LYP/6-31G(d) level (GAMESS[17]) the most electron deficient aromatic moieties participate in both 'best' (3-nitro-4-chloro) and 'worst' (3,5-dinitro) inhibitors (Fig. 6); it is possible that there is either

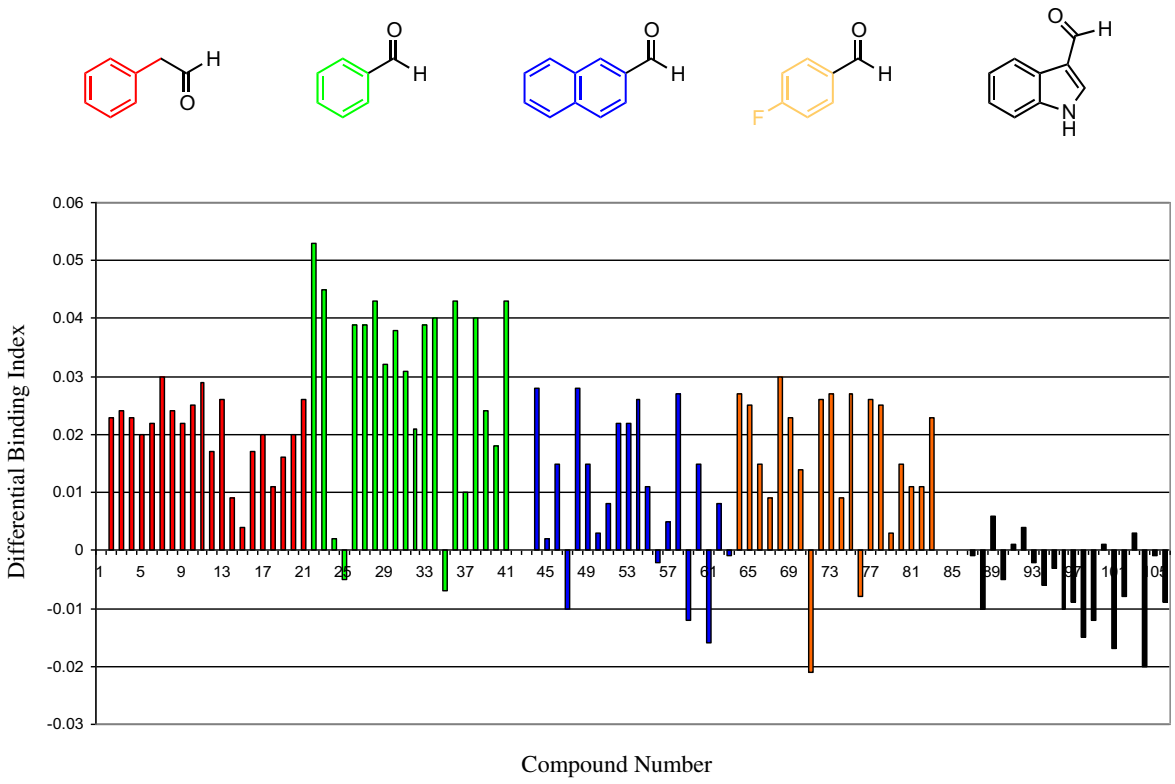

Fig. 3. Focused library screening results sorted by electron rich aromatic group.

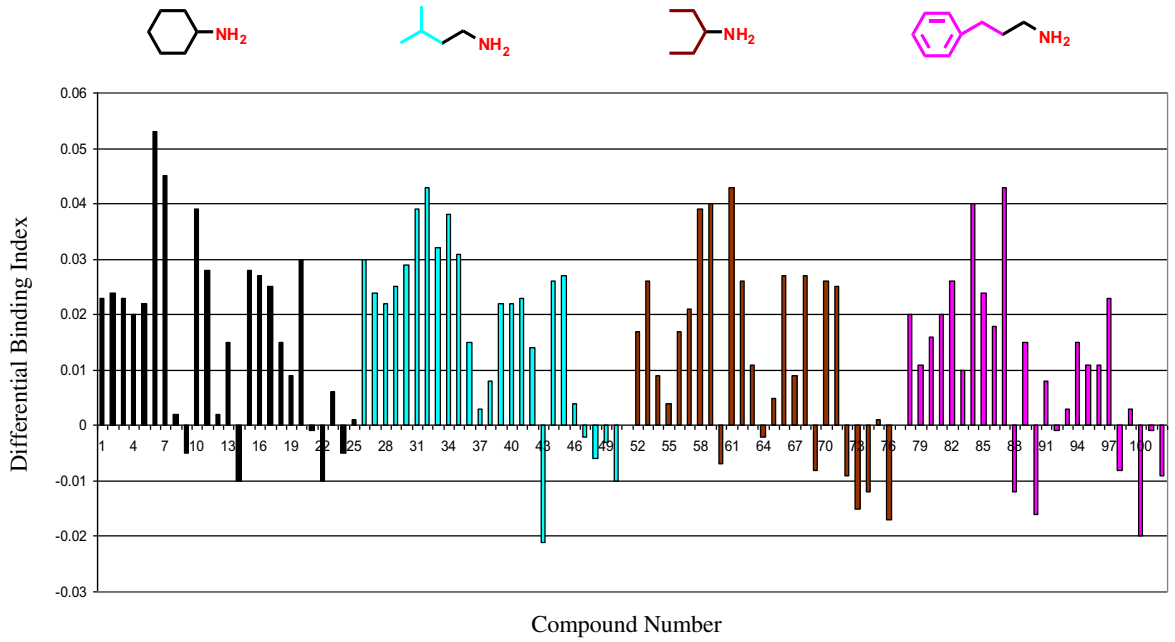

Fig. 4. Focused library screening results sorted by hydrophobic amine group.

a steric component to the selection in this case, or alternatively there is insufficient structural diversity to generate a strong SAR.

In an attempt to further understand SAR, hierarchical clustering of library compounds was conducted (Fig. 7; Tanimoto similarity >85%), which revealed additional insights for favorable RAGE binding. Compounds that contained both an indole electron rich aromatic and a mono or di-nitro electron deficient benzene were least favored for binding (cluster 1). Compounds containing mono or di-chloro substituted electron deficient benzenes with an indole electron rich aromatic were slightly less disfavored (cluster 3). The next most disfavored cluster (cluster 10) contained compounds with a naphthyl electron rich aromatic and a nitro containing electron deficient benzene. As with indole containing electron rich aromatic groups, naphthyl containing compounds performed better when paired with chloro containing electron deficient benzenes. Clusters with average differential binding indices near 0.01 all contained either naphthyl electron rich aromatics with chloro substituted electron deficient benzenes or nitro containing electron

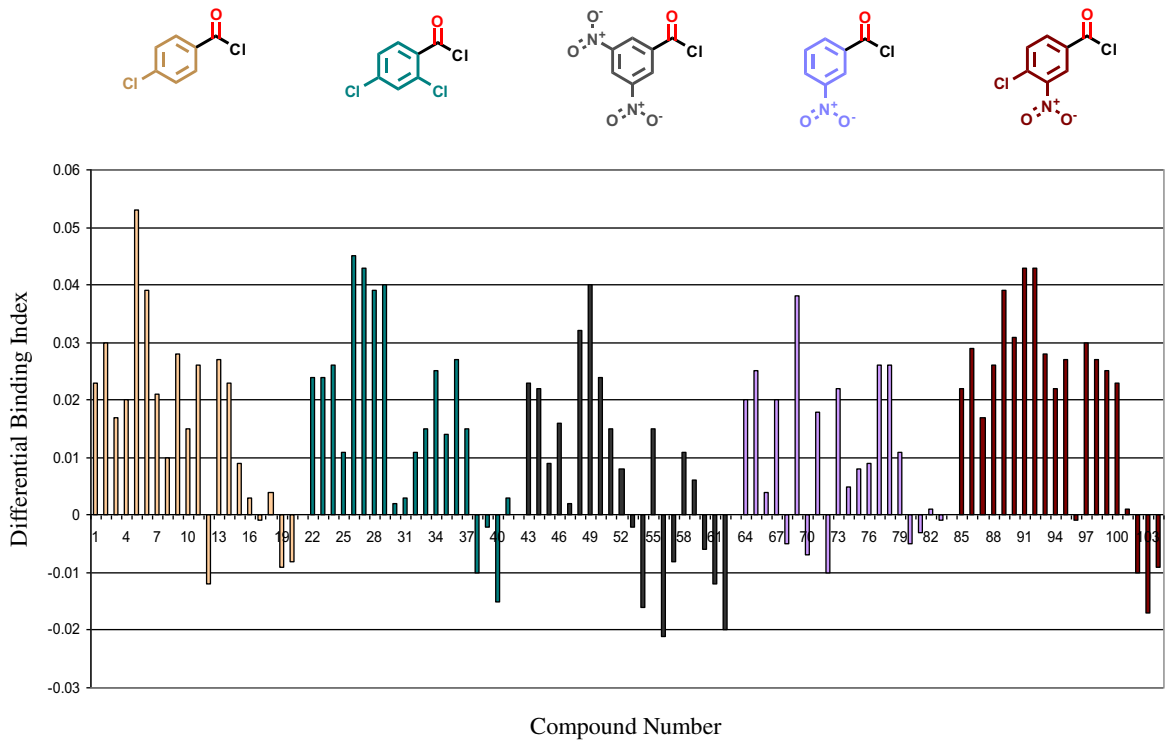

Fig. 5. Focused library screening results sorted by electron deficient benzene group.

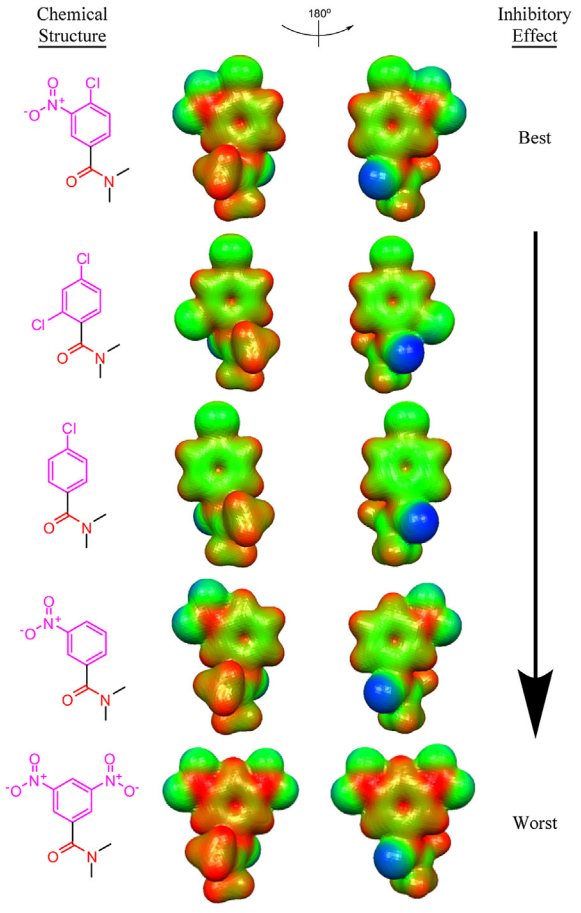

Fig. 6. Electrostatic potential maps of electron deficient benzene derivatives included in the focused library, visualized with MacMolPlt.[18] 'Best' and 'Worst' indicate the average inhibitory potency of library members incorporating these building blocks.

rich aromatics with any of benzyl, phenyl, or phenethyl electron rich aromatic groups (clusters 5, 7, 9, 17, and 19). Improved compound binding was observed for clusters that contained electron deficient benzenes with 3-nitro-4-chloro substitution (e.g., clusters 2 and 14) as well as compounds with dichloro substitution (e.g., clusters 4, 13, and 16). The best group (cluster 11), contains 3 compounds each with a *para*-chloro electron deficient benzene and a cyclohexyl hydrophobic amine (Fig. 8).

In an effort to determine if other molecular features could be correlated to compound activity, differential binding index values were compared against common 'drug-like' properties. The only significant correlation observed, while still quite weak, was between differential binding index and compound molecular weight (R^2=0.156; Supplemental Fig. 3), while all other properties compared were not significantly correlated (R^2<0.1) (rotatable bond count, amide count, atom count, H-bond donors, H-bond acceptors, polar surface area, and clogp).

A key goal in the library design was to reduce molecular weight, while retaining inhibitory potency. The average molecular weight of the three best commercial compounds tested in the original library screen was 521 Da. The average molecular weight of the five library members with best RAGE-Aβ inhibitory activity was 362 Da. The most active of these compounds weighs just 327 Da. As described elsewhere,[13] compound **1** showed a 52-fold increase in brain uptake in vivo relative to **4**, likely due at least in part to its reduced molecular weight. Compound **1** also inhibits RAGE-mediated influx of circulating Aβ40 and Aβ42 into the brain of aged $APP^{sw/0}$ mice, and normalizes their cognitive performance.

3. Conclusion

We have described the synthesis and analysis of a 100-compound focused library targeting inhibition of RAGE-Aβ binding. Results indicate that RAGE tolerates substantial structural variability within the context of the overall pharmacophore model; of the structures tested, those bearing an indole or nitro

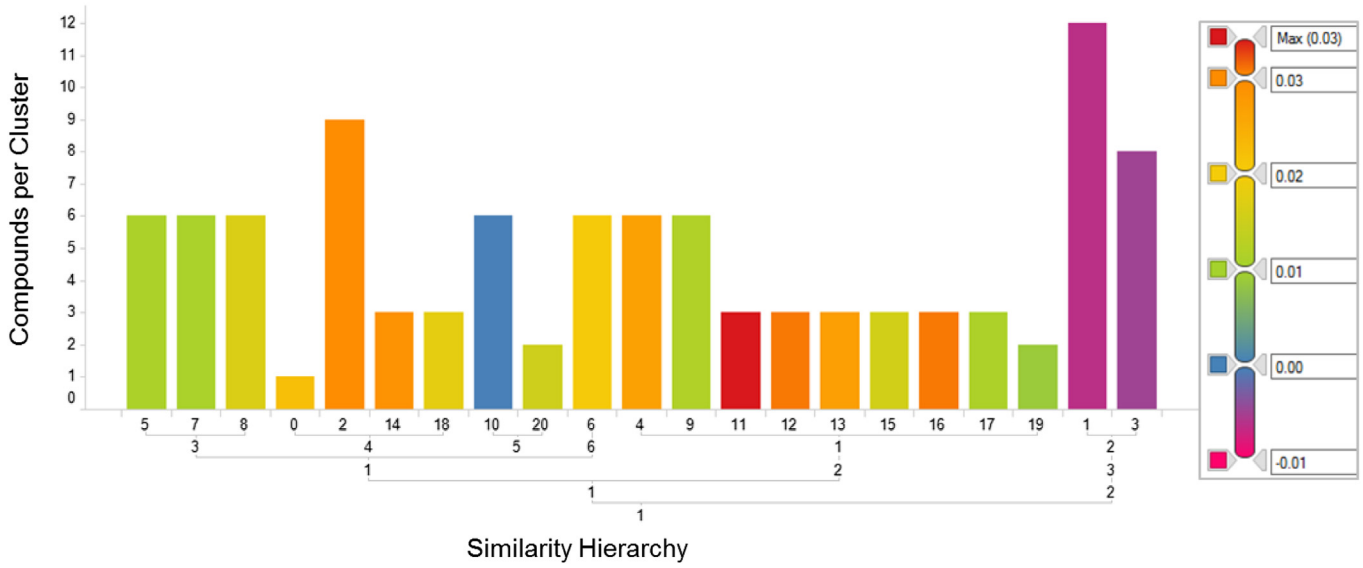

Fig. 7. Compounds clustered in groups with >85% structural similarity, bars colored by average differential binding index per cluster. Hierarchical clustering with Tanimoto similarities >85% reveals chemical features deleterious to effective RAGE binding.

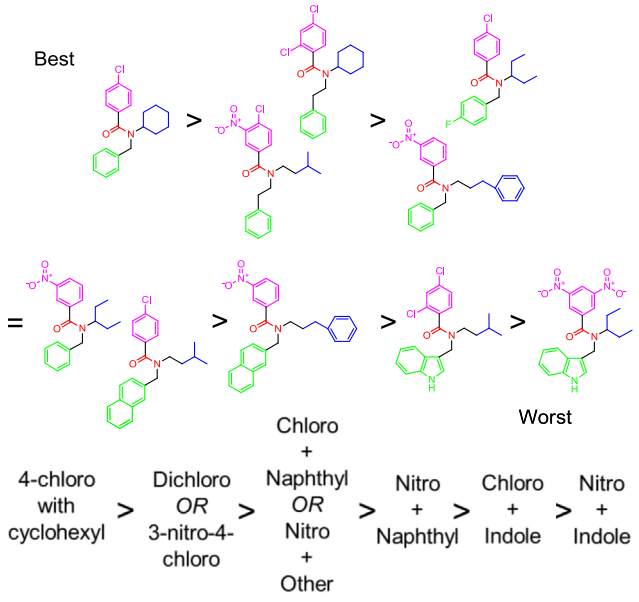

Fig. 8. Representative compounds from hierarchical clustering based upon Tanimoto similarities of >85% revealing features associated with binding.

substituted electron deficient benzenes were worse than the parent compounds, while phenyl electron rich aromatics and chloro substituted electron deficient benzenes were preferred. Given the broad range of targets bound by RAGE in vivo this promiscuity is perhaps unsurprising, and structural studies will be essential in order to understand the mode(s) of compound binding. While the in vivo activity of compound **1** is encouraging, significant work remains to produce a variant with better bioavailability. Efforts along those lines are in progress in our laboratories.

4. Experimental section

To generate the 100-compound focused library, Borch reductive amination[16] was used to combine hydrophobic primary amines with electron rich aromatic aldehydes to generate secondary amines. These secondary amines were then combined with electron deficient acid halides to produce the final tertiary amide library with the three desired peripheral groups. A representative synthesis is described below.

4.1. *N*-Benzyl-4-chloro-*N*-cyclohexylbenzamide (1)

To generate Compound **1**, cyclohexylamine (0.5 M in MeOH) was combined with benzaldehyde (0.5 M in MeOH) and stirred for 3 h at 64 °C. The mixture was cooled to rt, followed by two additions of sodium cyanoborohydride (0.5 M in EtOH), each followed by stirring at rt for 30 m. The mixture was then heated to 64 °C for 6 h. The reaction mixture was worked-up with water and extracted three times with CH_2Cl_2. The organic fractions were pooled, dried with magnesium sulfate, and reduced in vacuo. The secondary amine was then solubilized in dry CH_2Cl_2 and combined with 4-chlorobenzoylchloride. Equivalents were based upon the assumption that the secondary amine was formed in 100% yield. Dimethylaminopyridine (0.1 equiv) was solubilized in dry CH_2Cl_2 and added directly to the stirring solution of secondary amine, followed by addition of diisopropylethylamine (1.1 equiv). The reaction was then capped, purged with nitrogen gas, and stirred at rt overnight. The reaction mixture was then reduced in vacuo to an oil, which was resolubilized and purified using reverse phase preparative HPLC (isocratic elution: 75% acetonitrile, 25% water). Following preparative HPLC, compound purity was determined using reverse phase analytical HPLC. Compounds were purified to an average purity of greater than 95% (supplementary Table 1). For Compound **1**: IR (thin film from $CDCl_3$): 2935, 2858, 2246, 1624, 1495, 1418, 1091, 908, 838, 734 cm^{-1}; ^1H NMR (400 MHz, $CDCl_3$) δ 7.52 (4H), 7.36 (4H), 7.20 (2H), 4.55 (1H), 3.65 (1H), 1.80 (4H), 1.47 (4H), 1.06 (2H); ^{13}C NMR (75 MHz, $CDCl_3$) δ 171.2, 142.5, 139.0, 135.2, 128.7, 128.4, 127.7, 126.8, 77.17, 59.4, 59.4, 44.6, 32.0, 30.8, 25.7, 25.1, 25.1, 9.29; HRMS *m*/*z* calculated for (M+H); 328.1390, found: 328.1477.

4.2. Screening strategy

The ^{125}I-Aβ40 binding assay in RAGE-CHO cells was performed as reported.[13] First, RAGE-CHO cells were incubated at 4 °C for 3 h with ^{125}I-Aβ40 (5 nM) in the absence or presence of library members at a concentration of 10 μM. At the end of the incubation period the immobilized cells were washed with the cold non-radioactive

medium to remove ^{125}I-Aβ40, and lysed in a solution containing 1% NP-40 in 0.1 M NaCl at 37 °C for 15 min. The radioactivity was determined using 1470 Wallac Wizard (PerkinElmer, Meriden, CT) gamma counter. The fraction of ^{125}I-Aβ40 that was bound to the cell-surface RAGE was determined as previously reported.[13]

Acknowledgements

This work was supported by the ISOA/ADDF. We thank members of the former Center of Neurodegenerative and Vascular Brain Disorders (Department of Neurosurgery), University of Rochester, for their help.

Supplementary data

Supplementary data related to this article can be found at http://dx.doi.org/10.1016/j.tet.2013.05.079.

References and notes

1. Sosa-Ortiz, A. L.; Acosta-Castillo, I.; Prince, M. J. *Arch. Med. Res.* **2012**, *43*, 600–608.
2. Mayeux, R.; Stern, Y. *Cold Spring Harbor Perspect. Med.* **2012**, *2* a006239.
3. Walsh, D. M.; Selkoe, D. J. *J. Neurochem.* **2007**, *101*, 1172–1184.
4. Citron, M. *Nat. Rev. Drug Discovery* **2010**, *9*, 387–398.
5. Sankaranarayanan, S.; Price, E. A.; Wu, G.; Crouthamel, M. C.; Shi, X. P.; Tugusheva, K.; Tyler, K. X.; Kahana, J.; Ellis, J.; Jin, L.; Steele, T.; Stachel, S.; Coburn, C.; Simon, A. J. *J. Pharmacol. Exp. Ther.* **2008**, *324*, 957–969.
6. Dovey, H. F.; John, V.; Anderson, J. P.; Chen, L. Z.; de Saint Andrieu, P.; Fang, L. Y.; Freedman, S. B.; Folmer, B.; Goldbach, E.; Holsztynska, E. J.; Hu, K. L.; Johnson-Wood, K. L.; Kennedy, S. L.; Kholodenko, D.; Knops, J. E.; Latimer, L. H.; Lee, M.; Liao, Z.; Lieberburg, I. M.; Motter, R. N.; Mutter, L. C.; Nietz, J.; Quinn, K. P.; Sacchi, K. L.; Seubert, P. A.; Shopp, G. M.; Thorsett, E. D.; Tung, J. S.; Wu, J.; Yang, S.; Yin, C. T.; Schenk, D. B.; May, P. C.; Altstiel, L. D.; Bender, M. H.; Boggs, L. N.; Britton, T. C.; Clemens, J. C.; Czilli, D. L.; Dieckman-McGinty, D. K.; Droste, J. J.; Fuson, K. S.; Gitter, B. D.; Hyslop, P. A.; Johnstone, D. M.; Li, W. Y.; Little, S. P.; Mabry, T. E.; Miller, F. D.; Audia, J. E. *J. Neurochem.* **2001**, *76*, 173–181.
7. Schenk, D.; Barbour, R.; Dunn, W.; Gordon, G.; Grajeda, H.; Guido, T.; Hu, K.; Huang, J.; Johnson-Wood, K.; Khan, K.; Kholodenko, D.; Lee, M.; Liao, Z.; Lieberburg, I.; Motter, R.; Mutter, L.; Soriano, F.; Shopp, G.; Vasquez, N.; Vandevert, C.; Walker, S.; Wogulis, M.; Yednock, T.; Games, D.; Seubert, P. *Nature* **1999**, *400*, 173–177.
8. Wischik, C.; Bentham, P.; Wischik, D.; Seng, K. *Alzheimer's Dementia* **2008**, *4*, T167.
9. Khan, T. K.; Nelson, T. J.; Verma, V. A.; Wender, P. A.; Alkon, D. L. *Neurobiol. Dis.* **2009**, *34*, 332–339.
10. Neeper, M.; Schmidt, A. M.; Brett, J.; Yan, S. D.; Wang, F.; Pan, Y. C.; Elliston, K.; Stern, D.; Shaw, A. *J. Biol. Chem.* **1992**, *267*, 14998–15004.
11. Yan, S. D.; Chen, X.; Fu, J.; Chen, M.; Zhu, H.; Roher, A.; Slattery, T.; Zhao, L.; Nagashima, M.; Morser, J.; Migheli, A.; Nawroth, P.; Stern, D.; Schmidt, A. M. *Nature* **1996**, *382*, 685–691.
12. Deane, R.; Yan, S. D.; Submamaryan, R. K.; LaRue, B.; Jovanovic, S.; Hogg, E.; Welch, D.; Manness, L.; Lin, C.; Yu, J.; Zhu, H.; Ghiso, J.; Frangione, B.; Stern, A.; Schmidt, A. M.; Armstrong, D. L.; Arnold, B.; Liliensiek, B.; Nawroth, P.; Hofman, F.; Kindy, M.; Stern, D.; Zlokovic, B. *Nature Med.* **2003**, *9*, 907–913.
13. Deane, R.; Singh, I.; Sagare, A. P.; Bell, R. D.; Ross, N. T.; LaRue, B.; Love, R.; Perry, S.; Paquette, N.; Deane, R. J.; Thiyagarajan, M.; Zarcone, T.; Fritz, G.; Friedman, A. E.; Miller, B. L.; Zlokovic, B. V. *J. Clin. Invest.* **2012**, *122*, 1377–1392.
14. Han, Y. T.; Choi, G.-I.; Son, D.; Kim, N.-J.; Yun, H.; Lee, S.; Chang, D. J.; Hong, H.-S.; Kim, H.; Ha, H.-J.; Kim, Y.-H.; Park, H.-J.; Lee, J.; Suh, Y.-G. *J. Med. Chem.* **2012**, *55*, 9120–9155.
15. Lee, Y. S.; Kim, H.; Kim, Y.-H.; Roh, E. J.; Han, H.; Shin, K. J. *Bioorg. Med. Chem. Lett.* **2012**, *22*, 7555–7561.
16. Borch, R. F.; Bernstein, M. D.; Durst, H. D. *J. Am. Chem. Soc.* **1971**, *93*, 2897–2904.
17. GAMESS v22 Feb 2006 (R5) Schmidt, M. W.; Baldridge, K. K.; Boatz, J. A.; Elbert, S. T.; Gordon, M. S.; Jensen, J. H.; Koseki, S.; Matsunaga, N.; Nguyen, K. A.; Su, S.; Windus, T. L.; Dupuis, M.; Montgomery, J. A. J. *Comput. Chem.* **1993**, *14*, 1347–1363.
18. MacMolPlt v7.2.1 Bode, B. M.; Gordon, M. S. *J. Mol. Graphics Modeling* **1998**, *16*, 133–138.